What is surf-riding in irregular seas?

Kostas J. Spyrou , Nikos Themelis and Ioannis Kontolefas

School of Naval Architecture and Marine Engineering, National Technical University of Athens

Abstract: The concept of surf-riding in irregular seas is enquired and two calculation schemes are implemented in order to create upper and lower bounds of the probability of surf-riding. The first scheme is focused on the identification of the generation and disappearance of surge equilibria. Due to the time-varying nature of the dynamical system, these are finite-time objects, departing from the conventional notion of an equilibrium. The other scheme is aimed to determine time segments of ship motion where the mean speed is higher than expected. The probability values obtained by the two schemes are compared against each other and conclusions are drawn.

Key words: surf-riding; high-run; irregular waves;

1. Introduction

Phenomenologically, one could characterize as "surf-riding" a ship's prolonged run in waves with speed higher than the speed sustained by her propulsive thrust. For regular "seas" such behavior is owed to the generation of equilibrium conditions in the surge dynamics which create capture and a "push" of the ship on the down-slope of a steep wave. In irregular seas however, the meaning of an "equilibrium state" is questionable given the time-varying nature of system dynamics. Moreover, any plausible notion of ship dynamic equilibrium in surge could claim its relevance only for finite time segments during ship runs. One wonders therefore if what is established for regular seas could reasonably be extended to the irregular seas; and moreover, whether new phenomena distinctively identified with the time-varying nature of the system can also emerge.

In the current paper, the concept of "surf-riding equilibrium" in a multi-frequency wave field was enquired and a suitable scheme for the identification of such points was developed, involving calculation of the instantaneous celerity.

A numerical scheme was implemented for identifying these time segments in a long simulation record where the ship performs "high-runs" (she

moves with a mean velocity that is higher than the nominal). A massive campaign of simulations was subsequently performed for contrasting apparent surf-riding occurrences against equilibria existence.

2. Time segments of equilibria existence in multi-chromatic sea

2.1 Concept

Large-scale simulation results reveal finite time intervals over which instantaneous celerity (calculated at ship's position) and surge velocity, strongly relate to each other. Based on this, one could infer that some kind of point attractors can arise in the phase plane, advancing with velocity relating to the instantaneous celerity. These attractors (we will henceforth call them surf-riding equilibria for convenience) have finite life-spans over which they can invoke ship "high runs" if the ship is found within the basin of attraction of anyone of them.

To identify stable and unstable surf-riding equilibria in the vicinity of the ship, we introduce a non-inertial frame of reference that moves with the instantaneous celerity (it is evident that such equilibria will, in general, not constitute solutions of the surge equation; rather they lie inside bounded regions in the time-extended phase space that contain trajectories

qualified as "high-runs"). The ratio of the time that the scheme returns "positives" for the existence of equilibria, to the total time of exposure to a specified wave environment, should comprise an upper bound of the "probability of surf-riding".

2.2 Mathematical model and identification scheme

Consider the mathematical model of surge motion in following seas, written with respect to an earth-fixed observer, see for example [1]

$$
\begin{aligned}
\left(m-X_{\dot{u}}\right)\ddot{\xi} &+ \left(r_1-\tau_1 n\right)\dot{\xi} + \left(r_2-\tau_2\right)\dot{\xi}^2 \\
&+ r_3\dot{\xi}^3 - \sum_{i=1}^{N} f_i \sin\left(k_i\xi - \omega_i t + \varepsilon_i + \varepsilon_{fi}\right) = \tau_0 n^2
\end{aligned}
\tag{1}
$$

where ξ is the longitudinal position of the ship, m and $X_{\dot{u}}$ are her mass and "added mass" respectively, while n is the propeller rate. In the forcing term, k_i, ω_i and ε_i denote, respectively, the wave number, wave frequency and the random phase of the ω-harmonic component; f_i denote the amplitude and ε_{fi} the phase of the ω-harmonic wave force component.

Let us conceive a transformation that, in analogy to the one used for the harmonic case, would allow us to identify stationary points. This could be feasible if a new, non-inertial system of axes was introduced moving with the instantaneous celerity $c[\xi(t);t]$ at ship's position. Let us suppose that instantaneous celerity satisfies some appropriate smoothness conditions over some finite time interval (despite knowing that, the more the sea becomes "broad–banded", the more difficult will be to satisfy these conditions over such an interval). The location of the ship with respect to the new origin can be expressed by a new distance variable χ as follows,

$$
\chi = \xi - z
\tag{2}
$$

The variable z is the abscissa of the moving origin with respect to the earth - fixed frame, expressed as,

$$
z = z_0 + \int_{t_0}^{t} c\left[\xi(s);s\right]ds
\tag{3}
$$

For the existence of surf-riding equilibria the following condition must hold,

$$
\begin{aligned}
\sum_{i=1}^{N} f_i \sin&\left[k_i\left(\chi+z\right)-\omega_i t+\varepsilon_i+\varepsilon_{fi}\right]+\left(\tau_2 c^2+\tau_1 cn+\tau_0 n^2\right) \\
&-\left(r_1 c+r_2 c^2+r_3 c^3\right)-\left(m-X_{\dot{u}}\right)\dot{c} = 0
\end{aligned}
\tag{4}
$$

Should surf-riding equilibria be located, their paths are traced, under the condition however of remaining always within the close vicinity of the ship (only nearby equilibria pose a threat).

The ship selected for applying the above scheme is the ONR "tumblehome topside" that has been used in our previous studies ($L_{WL}=159$ m, $B_{WL}=18.802$ m, $T_{max}=7.605$ m) [2, 3]. A JONSWAP spectrum is assumed. It is discretized by applying a fixed frequency increment $\delta\omega=2\pi/t_{sim}$ where $t_{sim}=300\ s$ is the basis simulation time. To assess the effect of band-width, four scenarios are investigated in terms of the considered range around spectrum's peak. Several simulations were carried out, for parameters values shown below in Table 1.

Table 1 Parameters of the simulations carried out

Parameter	Value
u_{nom} (m/s)	(12,13)
$u(0)$ (m/s)	10
H_S (m)	(3,6)
T_P (s)	(9.5,10)
Considered range around ω_P (% ω_P)	(10,20,30,40)
Total simulation time T_{sim} (s)	1200

The detection scheme comprises of finding real roots of equation (4), if any, during the simulation, lying within a moving spatial window centered amidships, whose size is pre-specified and is used as a parameter of the investigation.

When a real root is detected, starting from a time instant let's say t_i and existing for n_i consecutive time steps, then the time interval $\left(t_i,\, t_i+\left(n_i-1\right)\delta t\right)$ represents a segment of existence of a threatening surf-riding equilibrium (nonetheless, it is not necessary the attraction to be felt by the ship and her motion to be affected). A time ratio of existence of equilibria is subsequently calculated by diving with the simulation time,

$$a = \frac{1}{T_{sim}}\sum_{i=1}^{N}\left(n_i-1\right)\delta t \qquad (5)$$

The results obtained are visualized in the form of animated series of figures (Fig. 1) in an attempt to gain better insight into the mechanism of "engagement to" and "disengagement from" surf-riding. We were able to recognize two different scenarios of entrapment,

1. The ship is initially attracted by the inset of an unstable equilibrium. Likewise regular sea scenarios, the trajectories in the neighborhood of this unstable state seem to be organized in such a way that the ship is engaged to a chase with the coexisting stable equilibrium.

2. A stable equilibrium appears suddenly in the close vicinity of the ship capturing her in the surf-riding condition.

In Fig.1 red circles correspond to equilibria identified using condition (3) while black circles correspond to roots of (3) when the last term of the lhs (accounting for the accelerating reference frame) is neglected. On the bottom part of these figures one can observe the time history of surge velocity (black line) versus that of instantaneous celerity calculated at ship's position (gray line).

## 3. Realizations of "high runs"

3.1 Definitions

In this part we have considered phenomenological realizations of surf-riding through simulation. Such events are evidenced by the up-crossing of a certain high velocity threshold and the later down-crossing of the same (or another selected) velocity threshold. In general, these two thresholds need not be identical and a subjective element is inevitable. Individual times of such events ("high runs) are summed up, then they are divided by the total time of the run in order to obtain the "time ratio of high run".

$$P_{\text{surf-riding}} = \frac{\sum_i t_{(i)\text{high-run}}}{T_{sim}} \qquad (6)$$

Two different specifications of the "high run" have been evaluated:

Definition 1: The two thresholds are identical and they are defined by the instantaneous celerity. In Fig. 2, such "high runs" are indicated by the dashed line arrows.

Definition 2: The threshold of up-crossing is the instantaneous celerity and the threshold of down-crossing is the nominal speed. This allows dealing with the fluctuations of the motion during surf-riding. This definition includes surge velocity fluctuations that may be below the instantaneous celerity but higher than nominal speed. Such time intervals are indicated in Fig. 2 with continuous line arrows. The condition the surge velocity to be higher than nominal speed is still invoked to exclude cases that qualitatively, should not qualify as high runs.
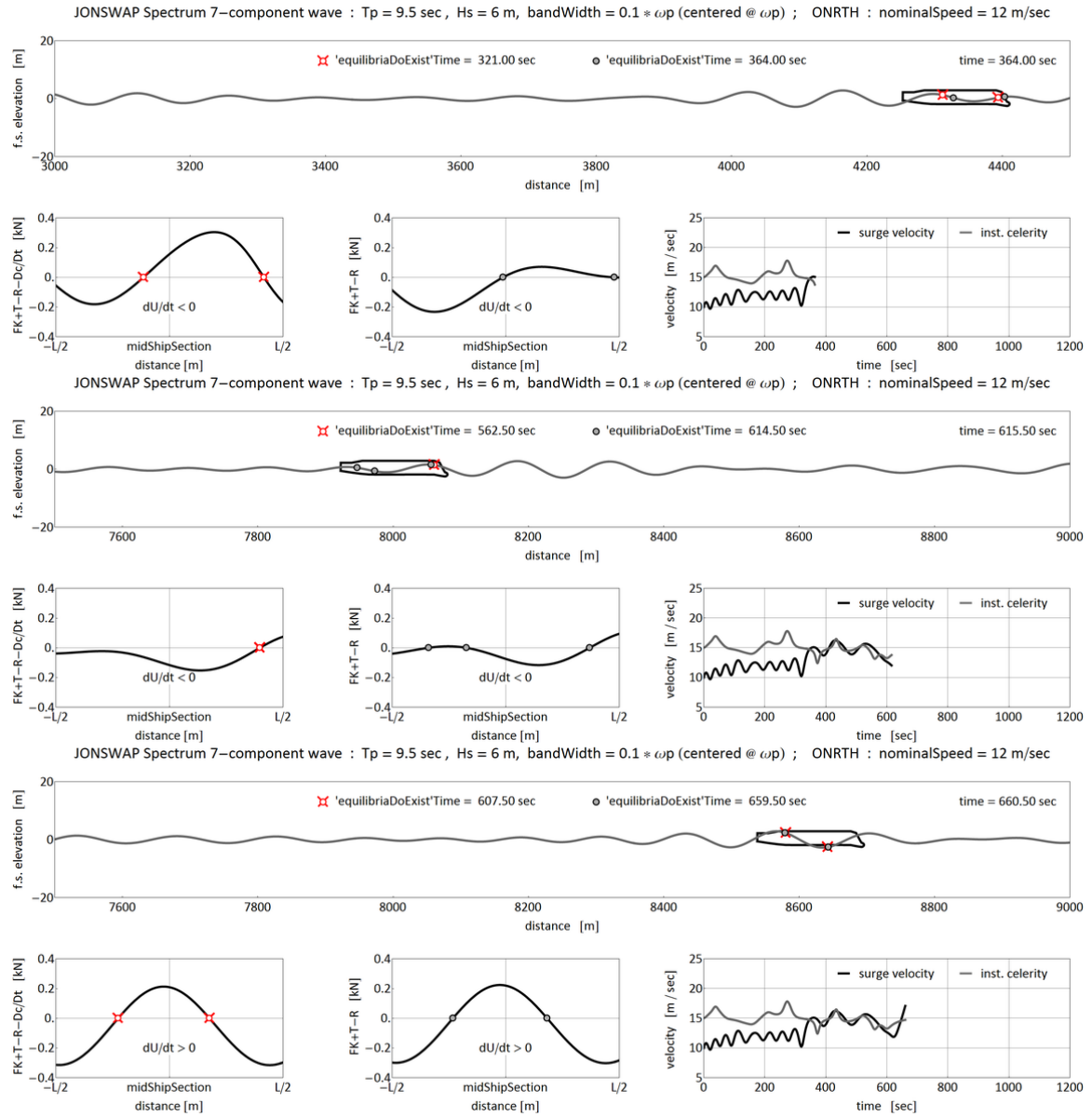
Fig. 1 - Time instants of an animated simulation [H_S=6 m, T_P=9.5 s, frequency range 10% ω_P (one side), u_{nom}=12m/s. The detection scheme was applied on a spatial window of one ship length.

3.2 Simulation settings

The simulation time was a multiple of the basis time $t_{sim} = 300$ s and specifically it was varied from t_{sim} to $40 \times t_{sim}$. Four ranges around spectrum's peak have been considered. Table 2 presents the considered ranges of the simulation parameters. Sensitivity

studies related to the sea state, narrowness of the spectrum and simulation time were carried out. The number of wave components that participate in the simulation (basis time) depends on the frequency range (Table 3). We run 100 wave realizations per scenario. The nominal and the initial speed of the ship in each scenario were unchanged (details are provided in [4]).

Table 2 Ranges of values of parameters

Parameter	Value
u_{nom} (m/s) - Fn	$12 - 0.308$
$u(0)$ (m/s)	10
wave realizations per scenario	100
H_S (m)	$(3 - 6)$
T_P (s)	$(8.5 - 13)$
(% ω_P one side)	$(5 - 30)$
Total simulation time T_{sim} (s)	$(t_{sim} - 40 \times t_{sim})$
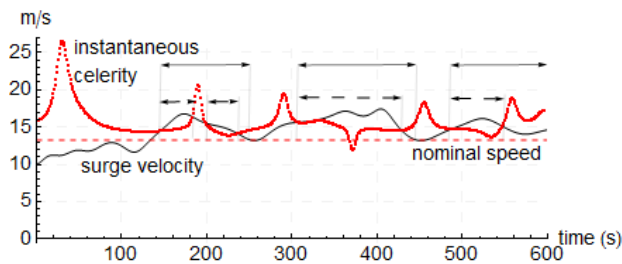
Fig. 2 – Schematic definitions of "high run".

3.2 Results

Fig. 3 shows time histories of surge velocity and instantaneous celerity for a "high-run" occurrence according to the 2nd definition. The lower diagram of Fig.3 shows the calculated time segments of "high-run". The convergence of the statistics was examined (see Fig. 4) and the simulation time per run was selected appropriately.

Effect of different "high run" definitions

In Fig. 5 are shown the obtained time ratios (loosely called "probabilities" although they can be regarded as such only in a crude sense) by varying the peak period and keeping constant the significant wave height. As expected, the first definition produces lower

probabilities than the second. There is significant influence on probability by a 10% increase of the down-crossing threshold.

**Table 3 Number of wave components per scenario for t_{sim} = 300 s.**

T_P (s)	5% ω_P	10% ω_P	20% ω_P	30% ω_P
8.5	4	8	15	22
9	4	7	14	21
9.5	4	7	13	19
10	4	7	13	19
10.5	3	6	12	18
11	3	6	11	17
11.5	3	6	11	16
12	3	6	11	16
12.5	3	5	10	15
13	3	5	10	14
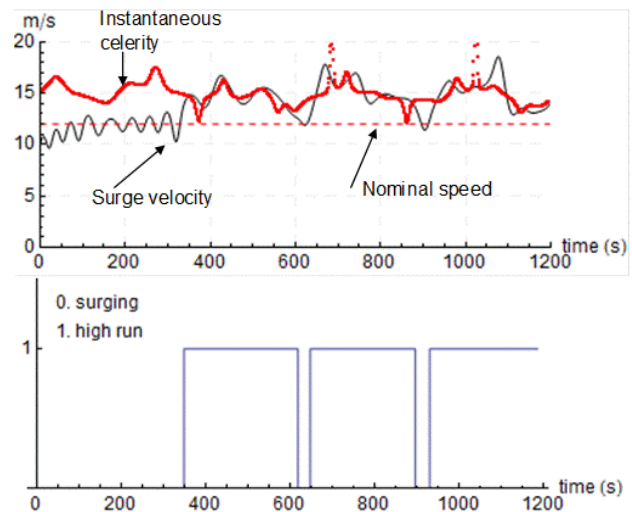
Fig. 3 – Sample simulation of a "high-run" and the respective time segments (low diagram) [H_S=6 m, T_P=9.5 s , u_{nom}=12m/s , frequency range 10% ω_P (one side)].
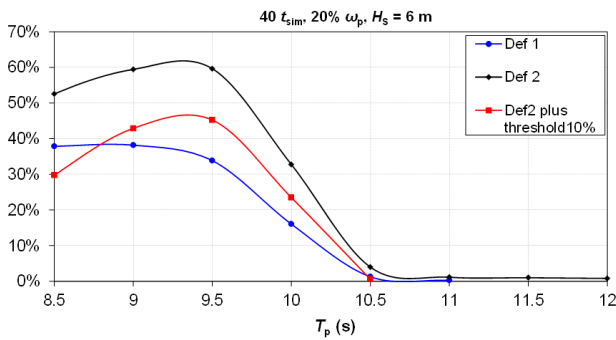
Fig. 4 – Probability of "high-run" (per definition) as function of the peak period T_P. The duration of the simulations was 40 t_{sim} = 12 x 103 s., the frequency range (one-side) was 20% ω_P and the significant wave height was H_S=6 m.
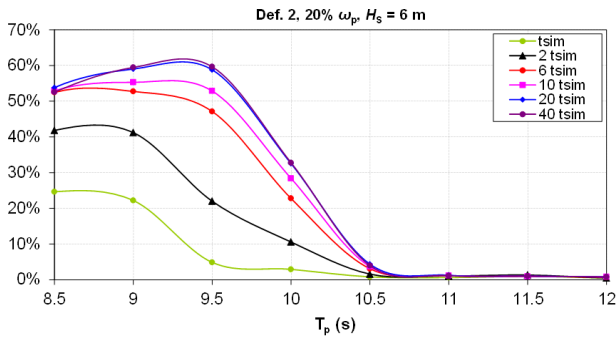
**Fig. 5 – Convergence of statistics per simulation time and varying T_P for 20% ω_P (one side), H_S=6 m.**

Effect of the frequency range

We have varied the peak period by keeping constant the significant wave height (Fig. 6). It was derived that in all cases, there is a peak period value below which there is sharp increase of the probability. By increasing the considered frequency range, high probabilities of surf-riding appear for a broader range.

3.3 Cross-comparison of calculated time ratios

A comparison study on the calculated time segments based on the methods of equilibria existence and "high runs" was carried out. Both results correspond to the same wave realizations, while a range of spatial window lengths (from $L/32$ up to

L, where L is the ship length) has been considered. Furthermore, four sea states and three frequency ranges were studied and the simulation time was fixed to $4 \times t_{sim}$.
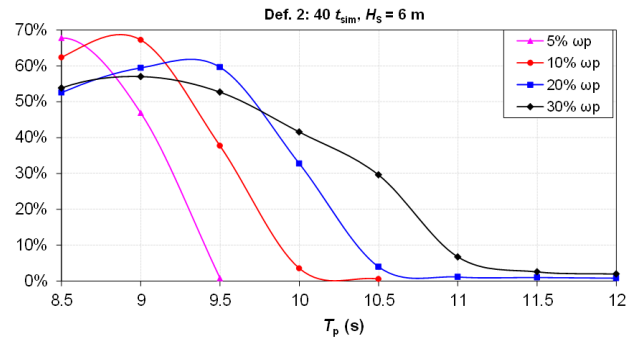

Fig. 6 - Probability of "surf-riding" (2nd definition) per % ω_P and varying T_P for 40 t_{sim} = 12 x 10^3 s, H_S=6 m.

The comparison results are summarized in Fig. 7. One can note a similar trend regarding the effect of the spatial window in the time ratios. However, higher differences are noted for the higher sea states.

Additionally, in Fig. 7 are included the time ratios according to the 2nd definition, but with a 10% increase of the down-crossing velocity threshold. As the time segments of equilibrium existence are not always felt by the ship, the two methods are not expected to produce directly comparable time-ratio results, a fact reflected by the diagrams.

4. Concluding remarks

The notion of surf-riding equilibrium was extended from the regular to a multi-chromatic sea where such "features" can exist for a finite time interval. A numerical scheme that is based on the concept of instantaneous celerity was developed to determine the time-ratio upper bound regarding the exposure to the danger of surf-riding. A more empirical approach for surf-riding prediction was subsequently applied, based on a campaign of numerical simulations, in order to calculate time intervals of 'high run.
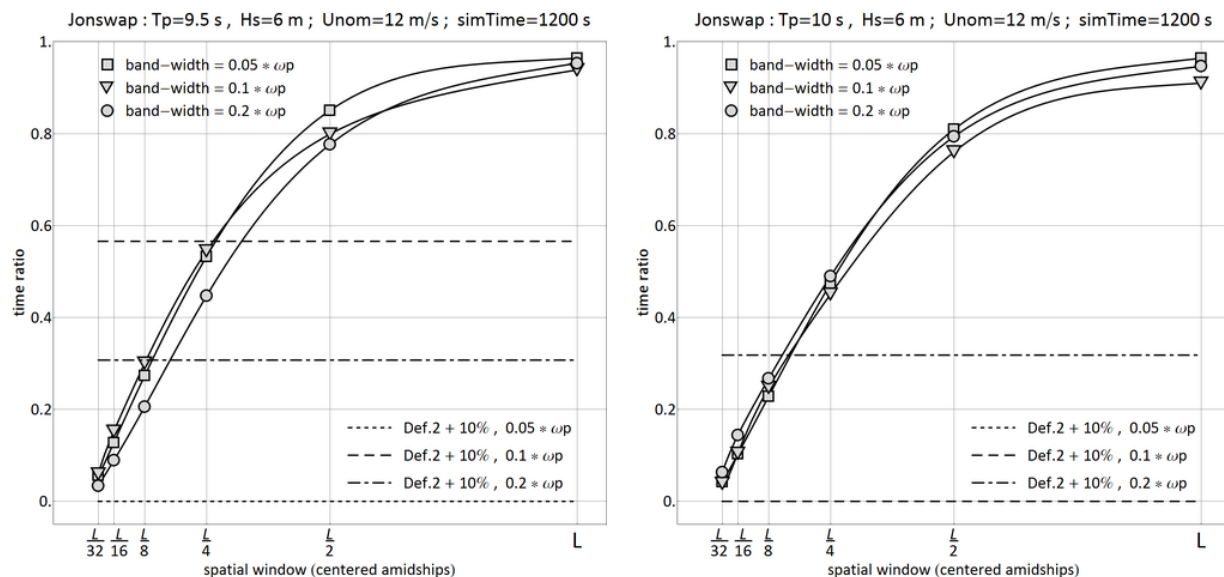
Fig. 7 - Effect of the different size of spatial windows on the upper bound of the time ratio of attraction to surf-riding and comparison with similar ratios corresponding to high runs.

Various up-crossing and down-crossing velocity thresholds that can determine a "high run" have been investigated. Statistical measures such as the mean time ratio and mean time duration of "high runs" were obtained. Moreover, sensitivity studies related to the sea state, narrowness of the spectrum and simulation time duration were carried out. Lastly, a preliminary comparison study on the time ratio of equilibrium existence and "high run" duration was performed, seeking a relation between these two quantities which, whilst related, they produce quantitatively very different time ratios of exposure to danger.

5. Acknowledgments

6. References

[1] K. Spyrou, V. Belenky, N. Themelis & K. Weems, Detection of Surf-riding Behavior of Ships in Irregular Seas, Nonlinear Dynamics, (2014) (accepted), DOI 10.1007/s11071-014-1466-2.

[2] K. Spyrou, V. Belenky, N. Themelis, K. Weems, Conditions of surf-riding in an irregular seaway, Proceedings, 11th International Conference on Stability of Ships and Ocean Vehicles, (2012), Athens, Greece.

[3] K. Spyrou, N. Themelis, Wave celerity in a multi-chromatic sea: a comparative study, Proceedings, 13th International Ship Stability Workshop, (2013), Brest, France.

[4] K. Spyrou, N. Themelis, I. Kontolefas, Development of Probabilistic Models for Evaluating the Dynamic Stability and Capsizing Tendency of Naval Vessels with Respect to Broaching-to, Technical Report to the Office of Naval Research (2014), ONRG grant number: N62909-13-1-7.